Dinuclear Ruthenium(II) and/or Osmium(II) Complexes of a Non-symmetric Bis-chelating Quaterpyridine Ligand. Synthesis, Electrochemical Behaviour, Absorption Spectra, Luminescence Properties and Intercomponent Energy Transfer†

Vincenzo Balzani,*[a] David A. Bardwell,[b] Francesco Barigelletti,*[c] Rosemary L. Cleary,[b] Massimo Guardigli,[c] John C. Jeffery,[b] Tiziana Sovrani[a] and Michael D. Ward*[b]
[a] *Dipartimento di Chimica 'Giacomo Ciamician', Università di Bologna, 40126 Bologna, Italy*
[b] *School of Chemistry, University of Bristol, Cantock's Close, Bristol BS8 1TS, UK*
[c] *Istituto FRAE-CNR, Via P. Gobetti 101, 40100 Bologna, Italy*

We have synthesized the hexafluorophosphate salts of the mono- and di-nuclear compounds Ru–LL′, Os–LL′, Ru–LL′–Ru, Os–LL′–Os, Ru–LL′–Os and Os–LL′–Ru, where Ru and Os are $\{Ru(bipy)_2\}^{2+}$ and $\{Os(bipy)_2\}^{2+}$ fragments (bipy = 2,2′-bipyridine), and LL′ is the bis-chelating 2,2′:3′,2″:6″,2‴-quaterpyridine bridging ligand with inequivalent bipy-type binding sites (L and L′). The compound $[(bipy)_2Os(LL')Ru(bipy)_2][PF_6]_4\cdot 3MeCN$ has been crystallographically characterized, the co-ordination environment about the Os^{II} centre is essentially identical to that of $[Os(bipy)_3]^{2+}$, but the co-ordination environment about the Ru^{II} centre is somewhat distorted with one particularly long Ru–N bond, due to the inherent sterically hindered nature of the L′ site of the bridging ligand. Electrochemical studies show that a given metal ion is slightly easier to oxidize when in the L co-ordination site, but the difference in the properties of the two moieties of the LL′ bridging ligand is much smaller than difference in the properties of Ru^{II} and Os^{II}, so that in the mixed-metal complexes Ru–LL′–Os and Os–LL′–Ru the metal easier to oxidize is always Os and the luminescent moiety is always the Os-based one. The lowest energy (luminescent) level in the homodinuclear compounds is located on the L co-ordination site. In Ru–LL′–Os and Os–LL′–Ru electronic energy transfer from the higher energy (Ru-based) to the lower energy (Os-based) moiety is very fast and 100% efficient.

The design and construction of supramolecular species capable of performing useful light-induced functions[1] requires the availability of molecular components having suitable chemical properties and appropriate geometrical structures. Because of their outstanding electrochemical and excited state properties,[2,3] ruthenium(II) and osmium(II) bipy-type complexes (bipy = 2,2′-bipyridine) are extensively used as building blocks for the construction of sensors[4,5] and light-harvesting[6] and charge-separation[7] devices. When such systems contain two or more metal-based units, the bridging ligands used to connect the metal centres are of crucial importance and fulfil three different functions. Firstly, the co-ordinating fragments at the termini of the bridging ligands must be appropriate for conferring the required electrochemical, photochemical and photophysical properties on the individual metal centres; in this area of chemistry we require bipy-type co-ordinating groups. Secondly, the shape and structure of the bridging ligand controls the structure of the supramolecular array, *i.e.* the overall spatial arrangement of the individual components. Thirdly, the nature of the groups linking the binding sites controls the extent of electronic communication between the building blocks. Thus, some workers have used flexible $-(CH_2)_n-$ chains to link the metal binding sites, although this has the disadvantage that conformational flexibility in solution means that structure–property correlations become difficult.[8] Direct coupling of two bipy-type units is an alternative.[9,10] With rigid, rod-like ligands containing spacers such as –HC=CH–bco–HC=CH–,[11] –C≡C–bco–C≡C– (bco = bicyclo[2.2.2]octane),[12] polyacetylenes such as –C≡C–C≡C–,[13] and *para*-linked phenyl rings[14] the separation between metal centres is fixed and the ligand conformation is limited, and photophysical properties such as energy-transfer rates may be correlated with metal–metal separation and the electronic nature of the bridging groups. Intramolecular energy-transfer from an excited Ru^{II} centre to a lower-energy Os^{II} centre has been a particular focus of attention, with efficiencies of above 90% occurring over distances of *ca.* 20 Å.[11,12,14]

In all of the cases reported so far, the two bipy co-ordination sites of the bridging ligand are equivalent, which implies the existence of only one L_2M–(bridging ligand)–$M'L_2$ positional isomer when two different metals M and M′ are used.‡ In contrast, we have been examining[16,17] the properties of luminescent mono- and di-nuclear complexes of the non-symmetric, bis-chelating bridging ligand 2,2′:3′,2″:6″,2‴-quaterpyridine,§ hereafter indicated by LL′ (Fig. 1). This has three differences from the series of rigid, rod-like ligands mentioned above. Firstly, the two chelating sites of LL′ are sterically and electronically non-equivalent, since (*i*) the co-ordination site of the 2,2′:3′ moiety (L) is unhindered for metal co-ordination,

---

† *Supplementary data available:* see Instructions for Authors, *J. Chem. Soc., Dalton Trans.*, 1995, Issue 1, pp. xxv–xxx.

‡ The non-symmetric 3,5-bis(pyridin-2-yl)-1,2,4-triazolate bis-chelating bridging ligand has previously been used to obtain homo- and hetero-dinuclear ruthenium and osmium complexes.[15]

§ In ref. 16 the bridging ligand was erroneously thought to be 2,2′:4′,2″:6″,2‴-quaterpyridine. The crystal structure obtained later for $[\{(CO)_3ClRe\}(LL')\{Ru(bipy)_2\}][PF_6]_2$ showed that the ligand is actually 2,2′:3′,2″:6″,2‴-quaterpyridine.[17]

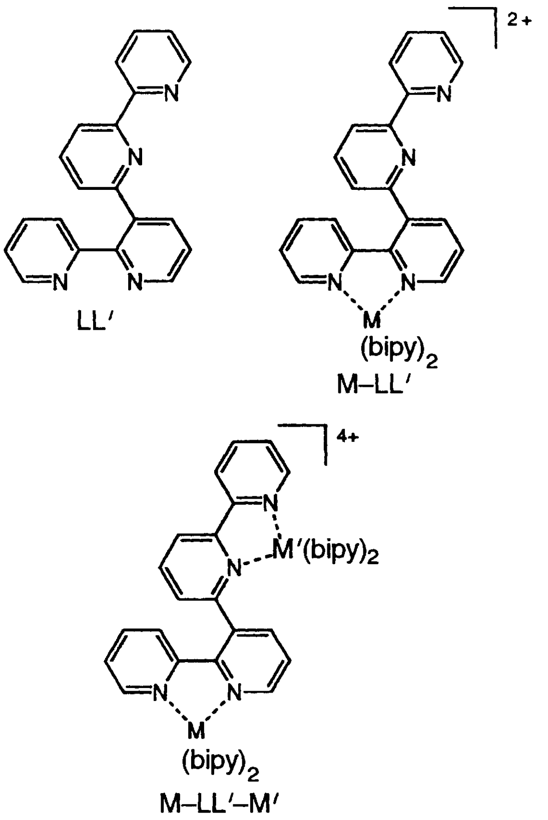

Fig. 1 Structural formulae of the bis-chelating 2,2':3',2'':6'',2'''-quaterpyridine bridging ligand LL' and of its mono- and di-nuclear metal complexes

whereas the co-ordination site of the 2'':6'',2''' moiety (L') is sterically crowded, and (*ii*) the two co-ordinating moieties each bear a 2,2'-bipyridyl substituent in different positions. Secondly, a substantial twist between the two halves of the ligand is necessary which removes most of the π–π overlap between the two components. Thirdly, the two binding sites are relatively close together. We have prepared the mono- and di-nuclear compounds Ru–LL', Os–LL', Ru–LL'–Ru, Os–LL'–Os, Ru–LL'–Os and Os–LL'–Ru (all as their hexafluorophosphate salts), where Ru and Os stand for $\{Ru(bipy)_2\}^{2+}$ and $\{Os(bipy)_2\}^{2+}$ (the terminal bipy ligands are not shown in the abbreviated formulae). The electrochemical properties, absorption spectra, and luminescence behaviour (emission spectra, excited-state lifetime, intercomponent energy transfer) of the prepared compounds are reported and discussed.

Results and Discussion

Synthesis and Characterization.—Syntheses of the mononuclear complexes Ru–LL' and Os–LL', and of the binuclear complexes Ru–LL'–Ru and Os–LL'–Os, were readily achieved by control of the metal: ligand ratio (slight excess of ligand for mononuclear complexes; > 2 equivalents of metal for binuclear complexes). In Ru–LL' and Os–LL' we assume that only the less-hindered 'external' binding site L of the ligand is occupied: the product isolated in each case was shown by ^1H NMR spectroscopy to be a single isomer and not a mixture of positional isomers. The electrochemical data are entirely consistent with this and further confirmation is provided by the crystal structure of Os–LL'–Ru (see below). The mixed-metal complex Ru–LL'–Os was prepared by reaction of Ru–LL' with $[Os(bipy)_2Cl_2]$, and the positional isomer Os–LL'–Ru was likewise prepared from Os–LL' and $[Ru(bipy)_2Cl_2]\cdot 2H_2O$. The complexes Ru–LL' and Ru–LL'–Ru have been prepared before;[16,17] analytical and FAB mass spectroscopic data for the other four complexes are in Table 1. The FAB mass spectra all show peaks corresponding to the expected mono- or bi-nuclear complex cations associated with varying numbers of $[PF_6]^-$ anions. All FAB peak clusters have the expected isotopic patterns.

The LL' bridging ligand cannot be planar because of steric effects. Molecular-modelling studies show that in the dinuclear compounds the two co-ordinating moieties of the bridging ligand have to be almost orthogonal. This was originally confirmed by the crystal structure of $[\{(CO)_3ClRe\}(LL')\{Ru(bipy)_2\}][PF_6]_2$ in which there is an 86° twist about the central C–C bond of the bridging ligand,[17] and is further confirmed by the crystal structure of Os–LL'–Ru (Fig. 2, Tables 2 and 3). The structural parameters of the Os^{II} centre, at the less hindered L site of the bridging ligand, are very similar to those of $[Os(bipy)_3]^{2+}$ (Os–N 2.056 Å)[18] with all bond lengths in the range 2.05–2.07 Å and all bite angles typical for chelating bipyridines. The chelating bipy fragment L of the bridging ligand has a twist of *ca.* 13° between the two pyridyl rings due to the presence of the bulky substitutent at the C^3 position of one of them. The more hindered nature of site L' is shown by the fact that whereas five of the Ru–N bond lengths lie in the typical range of 2.05–2.07 Å {*cf.* 2.056 Å for $[Ru(bipy)_3]^{2+}$},[19] the Ru(1)–N(61) bond involving the pyridyl ring of the bridging ligand which is adjacent to the bulky substitutent, has a length of 2.137(9) Å. This distortion of the co-ordination sphere of the metal at site L' is similar to that seen in $[\{(CO)_3ClRe\}(LL')\{Ru(bipy)_2\}][PF_6]_2$.[17] The torsion angle between the two halves of the bridging ligand is again 86°. A significant feature of the structure is the presence of aromatic π-stacking interactions between the two components. One of the bipy ligands attached to the Ru^{II} centre overlaps with the external bipy binding site L of the bridging ligand attached to the Os^{II} centre. The two overlapping aromatic segments are not parallel; within the overlapping region the inter-planar distance varies between 3 and 4 Å. The Ru ••• Os distance is 7.16 Å.

Since the complex contains two chiral centres there are four possible stereoisomers, *i.e.* two pairs of diastereoisomers. The complex crystallises in the space group $P2_1/n$, and only one pair of enantiomers is present in the crystal. This suggests one of two things: (*i*) addition of the second metal fragment at site L' is controlled by the chirality present at site L for steric reasons, so one diastereoisomer preferentially forms; (*ii*) there is no chiral control, so all possible stereoisomers form, but the two diastereoisomers may crystallise differently. The different diastereoisomers were examined by molecular modelling (the molecular mechanics programme in the CAChe package).[20] The configuration of the external Os^{II} centre was kept the same but the configuration of the internal Ru^{II} centre was varied by altering the points of attachment of the two bipy ligands; the structures were then energy-minimised using MM2 parameters. In one case the minimum-energy conformation approximated closely to that of the crystal structure, with a substantial area of π overlap between a bipy ligand attached to Ru^{II} and the L bipy fragment of the bridging ligand attached to Os^{II}. When the configuration of the Ru^{II} centre was reversed this stacking interaction largely disappeared, since the bipy ligand on the Ru^{II} which participated in the interaction is moved away from fragment L of the bridging ligand with which it previously stacked; this structure was computed to be the less stable of the two by *ca.* 10 kJ mol^{-1}. It is possible that both diastereoisomers are formed during the attachment of a chiral metal fragment at site L, but the product we obtained behaved as a single compound during chromatography. Proton NMR spectroscopy was unhelpful due to the presence of large numbers of overlapping signals (46 inequivalent aromatic protons *per* diastereoisomer). We note simply that both of the crystals we examined were found to contain only the diastereoisomer in which the π- stacking is more prevalent and which is predicted to have the lower energy of the two. Similar behaviour was observed for $[\{(CO)_3ClRe\}(LL')\{Ru(bipy)_2\}][PF_6]_2$ which likewise formed crystals containing only one pair of enantiomers.[17]

Table 1 Analytical and mass spectroscopic data for the new complexes

	Analysis (%)*			FAB mass spectra	
Complex	C	H	N	*m/z**	Assignment
$[Os(LL')(bipy)_2][PF_6]_2 \cdot 0.5C_7H_8$	45.8 (45.8)	3.2 (3.0)	9.8 (9.7)	1113 (1111)	$\{Os(LL')(bipy)_2(PF_6)_2\}$
				959 (959)	$\{Os(LL')(bipy)_2(PF_6)\}$
				814 (814)	$\{Os(LL')(bipy)_2\}$
				657 (658)	$\{Os(LL')(bipy)\}$
$[(bipy)_2Os(LL')Os(bipy)_2][PF_6]_4$	37.8 (38.0)	2.6 (2.4)	8.9 (8.9)	1754 (1753)	$\{[Os(bipy)_2]_2(LL')(PF_6)_3\}$
				1606 (1608)	$\{[Os(bipy)_2]_2(LL')(PF_6)_2\}$
				1462 (1463)	$\{[Os(bipy)_2]_2(LL')(PF_6)\}$
				1316 (1318)	$\{[Os(bipy)_2]_2(LL')\}$
$[(bipy)_2Ru(LL')Os(bipy)_2][PF_6]_4$	39.5 (39.9)	2.6 (2.5)	9.6 (9.3)	1663 (1663)	$\{(bipy)_2Ru(LL')Os(bipy)_2(PF_6)_3\}$
				1515 (1518)	$\{(bipy)_2Ru(LL')Os(bipy)_2(PF_6)_2\}$
				1372 (1373)	$\{(bipy)_2Ru(LL')Os(bipy)_2(PF_6)\}$
$[(bipy)_2Os(LL')Ru(bipy)_2][PF_6]_4 \cdot MeCN$	40.4 (40.3)	2.6 (2.7)	10.2 (9.9)	1662 (1663)	$\{(bipy)_2Os(LL')Ru(bipy)_2(PF_6)_3\}$
				1515 (1518)	$\{(bipy)_2Os(LL')Ru(bipy)_2(PF_6)_2\}$
				1371 (1373)	$\{(bipy)_2Os(LL')Ru(bipy)_2(PF_6)\}$

* Calculated values in parentheses.

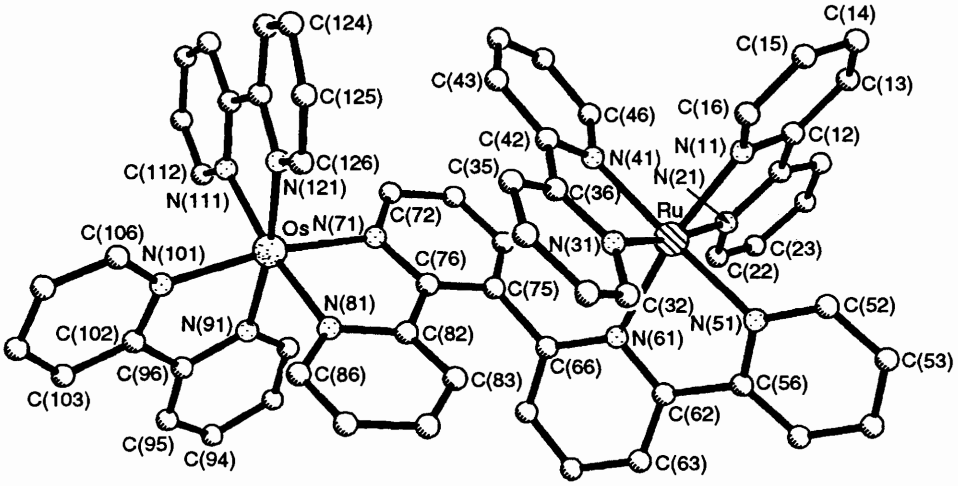

Fig. 2 Crystal structure of $[(bipy)_2Os(LL')Ru(bipy)_2]^{4+}$

Electrochemical Behaviour.—The results obtained by cyclic voltammetry and square-wave voltammetry experiments are gathered in Table 4; the results obtained under the same conditions for $[Ru(bipy)_3]^{2+}$ and $[Os(bipy)_3]^{2+}$ are also shown for comparison purposes. Oxidation of Ru–LL' and Os–LL' is reversible and takes place at potentials very close to those of the prototype complexes $[Ru(bipy)_3]^{2+}$ and $[Os(bipy)_3]^{2+}$, showing that the mono-co-ordinated LL' bridging ligand exhibits electron donor–acceptor properties very similar to those of bipy. Both mononuclear compounds also show three reversible, well separated, one-electron reduction waves similar to those of $[Ru(bipy)_3]^{2+}$ and $[Os(bipy)_3]^{2+}$, respectively. In both cases the first reduction wave takes place at a slightly less negative potential than in the prototype compound, suggesting that this process might involve the bridging ligand.

The electrochemical properties of homodinuclear Ru–LL'–Ru have been discussed in our previous paper,[17] and exactly the same arguments apply to Os–LL'–Os which behaves in the same way, showing two closely-spaced metal-centred oxidations. This can be due to the non-equivalence of the two co-ordination sites of the bridging ligand and/or to a non-negligible electronic interaction between the two metal centres, expected because of the short metal–metal separation. The first oxidation process occurs at a more positive potential compared with that of the parent mononuclear compound, which is to be expected considering the higher overall charge on the binuclear complexes (+4 instead of +2). Two distinct oxidation processes also occur for the two isomeric heterodinuclear Ru–LL'–Os and Os–LL'–Ru compounds. Comparison with the data obtained for the other compounds (Table 4) clearly shows that in both cases the first oxidation is the Os^{II}–Os^{III} couple and the second one is the Ru^{II}–Ru^{III} couple. Comparison of the metal-based redox potentials of the isomeric mixed-metal complexes Ru–LL'–Os and Os–LL'–Ru allows determination of the extent to which the asymmetry of the binding sites contributes to the electrochemical behaviour. Thus, the Ru^{II} centre oxidizes at +1.05 V (*vs.* ferrocene–ferrocenium) when at site L but at +1.09 V when at site L'. Similarly the Os^{II} centre oxidises at +0.57 V when at site L and at +0.60 V when at site L'. We may conclude that a metal is slightly easier to oxidize when it occupies the L co-ordination site of the bridging ligand. The difference imposed on the oxidation potentials by the inequivalence of the binding sites of LL' is, however, much smaller than the intrinsic difference between the Ru^{II}–Ru^{III} and Os^{II}–Os^{III} redox potentials.

In all four dinuclear complexes, the first reduction process takes place at a potential much less negative than that of the parent mononuclear complex, showing that this first process concerns the bridging ligand whose effective electron density decreases upon co-ordination to the second metal centre. The less negative first-reduction potential of Os–LL'–Os compared with Ru–LL'–Ru is related to the better ability of Os to delocalise the electric charge, a phenomenon that can also be

Table 2 Atomic coordinates (× 10^4) for $[(bipy)_2Os(LL')Ru(bipy)_2][PF_6]_4\cdot3MeCN$

Atom	*x*	*y*	*z*	Atom	*x*	*y*	*z*
Os	1 848(1)	2 502(1)	1 311(1)	N(101)	2 924(6)	2 436(4)	1 028(6)
Ru	−866(1)	3 999(1)	2 891(1)	C(102)	2 885(8)	2 500(6)	267(9)
N(11)	−1 031(7)	3 924(4)	4 005(7)	C(103)	3 573(10)	2 513(7)	−1(10)
C(12)	−1 813(11)	3 877(6)	4 015(9)	C(104)	4 298(10)	2 443(8)	546(14)
C(13)	−2 016(12)	3 866(6)	4 725(11)	C(105)	4 338(9)	2 365(8)	1 315(12)
C(14)	−1 414(15)	3 911(7)	5 435(11)	C(106)	3 636(9)	2 361(6)	1 531(10)
C(15)	−641(14)	3 941(7)	5 419(10)	N(111)	1 723(6)	1 690(4)	1 342(6)
C(16)	−467(10)	3 953(5)	4 698(8)	C(112)	1 417(8)	1 371(6)	732(8)
N(21)	−2 089(6)	3 855(4)	2 589(6)	C(113)	1 282(9)	826(6)	794(10)
C(22)	−2 596(8)	3 822(5)	1 865(9)	C(114)	1 479(10)	625(7)	1 537(11)
C(23)	−3 404(9)	3 755(7)	1 715(11)	C(115)	1 790(10)	926(7)	2 189(10)
C(24)	−3 733(12)	3 735(9)	2 296(14)	C(116)	1 903(8)	1 459(5)	2 062(8)
C(25)	−3 229(12)	3 770(8)	3 083(14)	N(121)	2 320(6)	2 343(5)	2 510(6)
C(26)	−2 389(10)	3 820(6)	3 238(10)	C(122)	2 242(8)	1 836(5)	2 739(8)
N(31)	349(6)	4 087(4)	3 317(5)	C(123)	2 496(9)	1 681(7)	3 519(8)
C(32)	753(9)	4 548(6)	3 397(8)	C(124)	2 867(10)	2 056(7)	4 089(9)
C(33)	1 567(10)	4 590(8)	3 739(10)	C(125)	2 994(8)	2 552(6)	3 841(8)
C(34)	2 007(11)	4 137(8)	3 970(12)	C(126)	2 672(9)	2 689(7)	3 058(10)
C(35)	1 616(10)	3 656(7)	3 881(9)	P(1)	−3 141(2)	2 169(2)	1 096(3)
C(36)	778(8)	3 629(6)	3 525(7)	F(1)	−2 588(8)	2 597(5)	1 533(11)
N(41)	−507(6)	3 216(4)	3 078(5)	F(2)	−3 613(8)	2 026(9)	1 642(8)
C(42)	293(14)	3 139(5)	3 419(7)	F(3)	−2 670(9)	2 238(8)	461(10)
C(43)	605(10)	2 635(6)	3 653(9)	F(4)	−3 659(9)	1 739(6)	529(8)
C(44)	93(14)	2 213(7)	3 573(9)	F(5)	−2 512(7)	1 742(5)	1 470(10)
C(45)	−697(12)	2 283(6)	3 226(9)	F(6)	−3 762(7)	2 579(5)	685(12)
C(46)	−991(9)	2 780(5)	2 999(7)	P(2)	4 361(3)	905(2)	2 960(2)
N(51)	−1 192(6)	4 796(4)	2 795(6)	F(7)	5 101(7)	1 007(4)	3 696(6)
C(52)	−1 338(9)	5 086(6)	3 388(9)	F(8)	4 519(7)	293(4)	3 150(7)
C(53)	−1 685(11)	5 582(7)	3 258(11)	F(9)	4 888(7)	858(7)	2 400(7)
C(54)	−1 900(10)	5 789(6)	2 503(11)	F(10)	3 792(8)	890(6)	3 497(7)
C(55)	−1 730(9)	5 495(6)	1 916(10)	F(11)	3 623(6)	782(6)	2 240(7)
C(56)	−1 380(7)	5 002(5)	2 057(8)	F(12)	4 180(10)	1 488(5)	2 797(11)
N(61)	−841(5)	4 184(4)	1 707(5)	F(13)	9 349(9)	1 598(7)	8 070(10)
C(62)	−1 128(7)	4 678(5)	1 479(7)	F(14)	8 547(7)	1 065(7)	8 385(9)
C(63)	−1 168(8)	4 872(6)	722(8)	P(3)	9 466(3)	1 107(3)	8 616(4)
C(64)	−926(8)	4 574(6)	185(8)	F(15)	9 434(9)	1 463(6)	9 332(9)
C(65)	−615(7)	4 094(6)	431(7)	F(16)	9 514(11)	762(7)	7 924(9)
C(66)	−577(7)	3 891(5)	1 169(7)	F(17)	10 371(6)	1 185(7)	8 861(8)
N(71)	730(5)	2 671(4)	1 438(5)	F(18)	9 549(9)	624(6)	9 181(9)
C(72)	165(8)	2 293(5)	1 425(7)	P(4)	−3 472(4)	4 510(3)	−456(4)
C(73)	−623(8)	2 429(6)	1 349(7)	F(19)	−2 900(10)	4 049(7)	−20(9)
C(74)	−834(7)	2 943(5)	1 309(7)	F(20)	−4 009(10)	4 949(7)	−951(12)
C(75)	−267(6)	3 340(5)	1 358(6)	F(21)	−2 831(8)	4 589(5)	−928(8)
C(76)	533(7)	3 195(5)	1 439(6)	F(22)	−3 047(9)	4 905(9)	185(11)
N(81)	1 883(6)	3 319(4)	1 406(6)	F(23)	−3 866(8)	4 091(6)	−1 113(11)
C(82)	1 194(6)	3 567(5)	1 498(7)	F(24)	−4 123(11)	4 389(10)	−56(12)
C(83)	1 187(7)	4 100(5)	1 634(7)	N(201)	−5 936(32)	4 935(19)	−1 876(44)
C(84)	1 855(8)	4 410(5)	1 673(9)	C(202)	−5 821(27)	4 529(17)	−2 054(31)
C(85)	2 526(8)	4 159(6)	1 544(10)	C(203)	−5 663(30)	4 023(16)	−2 316(29)
C(86)	2 533(8)	3 627(5)	1 427(9)	N(301)	−3 168(21)	6 286(12)	736(21)
N(91)	1 475(6)	2 579(4)	88(6)	C(302)	−3 678(21)	6 185(11)	249(18)
C(92)	735(9)	2 633(6)	−355(9)	C(303)	−4 373(16)	6 056(15)	−364(22)
C(93)	527(11)	2 716(8)	−1 169(10)	N(401)	−6 999(21)	4 979(14)	−4 290(26)
C(94)	1 133(14)	2 733(10)	−1 524(10)	C(402)	−6 470(24)	4 718(17)	−4 208(29)
C(95)	1 888(12)	2 668(8)	−1 085(9)	C(403)	−5 864(30)	4 337(21)	−4 050(33)
C(96)	2 081(9)	2 593(6)	−280(8)				

observed in the mononuclear compounds. The second reduction potentials of Ru–LL′–Ru and Os–LL′–Os are again less negative than the second reduction potential of the corresponding mononuclear compounds, and are almost coincident with the first reduction potentials of the corresponding tris-bipy complexes. It should also be noticed that the third reduction potential is much closer to the second one than in the mononuclear compounds. This behaviour is consistent with the assignment of the second reduction process to a bipy ligand belonging to the metal that involves the non-reduced moiety of the bridging ligand, and the third reduction process to a bipy ligand co-ordinated to the metal that involves the reduced bipy fragment of LL′.

The reduction potentials of the Ru–LL′–Os and Os–LL′–Ru heterodinuclear isomers are generally similar and fit well with those of the parent homonuclear complexes.

Absorption Spectra.—The wavelengths of the maxima of the absorption spectra are reported in Table 5. The absorption spectra of Ru–LL′–Os and Os–LL′–Ru are shown in Fig. 3. The absorption spectra are dominated in the UV region by very intense bands assigned to spin-allowed, ligand-centred (l.c.) transitions, and by moderately intense bands in the visible region assigned to spin-allowed metal-to-ligand charge-transfer (m.l.c.t.) transitions. For the osmium compounds, weaker, formally spin-forbidden, m.l.c.t. bands can also be observed in the low energy region of the visible spectrum.

The visible absorption spectra of the mononuclear M–LL′

Table 3 Selected bond lengths (Å) and angles (°) for $[(bipy)_2Os(LL')Ru(bipy)_2][PF_6]_4\cdot 3MeCN$

Os-N(111)	2.051(10)	Ru-N(31)	2.047(10)
Os-N(81)	2.056(10)	Ru-N(11)	2.056(10)
Os-N(71)	2.059(9)	Ru-N(41)	2.058(10)
Os-N(91)	2.067(10)	Ru-N(51)	2.073(10)
Os-N(121)	2.069(11)	Ru-N(21)	2.072(10)
Os-N(101)	2.070(10)	Ru-N(61)	2.137(9)
N(111)-Os-N(81)	171.5(4)	N(31)-Ru-N(11)	93.8(4)
N(111)-Os-N(71)	95.2(4)	N(31)-Ru-N(41)	78.9(4)
N(81)-Os-N(71)	78.1(4)	N(11)-Ru-N(41)	83.0(4)
N(111)-Os-N(91)	96.6(4)	N(31)-Ru-N(51)	99.0(4)
N(81)-Os-N(91)	89.1(4)	N(11)-Ru-N(51)	93.4(4)
N(71)-Os-N(91)	93.4(4)	N(41)-Ru-N(51)	175.7(4)
N(111)-Os-N(121)	78.3(4)	N(31)-Ru-N(21)	172.8(4)
N(81)-Os-N(121)	96.6(4)	N(11)-Ru-N(21)	79.8(5)
N(71)-Os-N(121)	92.9(4)	N(41)-Ru-N(21)	96.8(4)
N(91)-Os-N(121)	172.3(4)	N(51)-Ru-N(21)	84.8(4)
N(111)-Os-N(101)	92.1(4)	N(31)-Ru-N(61)	91.8(4)
N(81)-Os-N(101)	95.2(4)	N(11)-Ru-N(61)	170.2(4)
N(71)-Os-N(101)	169.8(4)	N(41)-Ru-N(61)	106.0(3)
N(91)-Os-N(101)	78.7(4)	N(51)-Ru-N(61)	77.8(4)
N(121)-Os-N(101)	95.6(4)	N(21)-Ru-N(61)	95.0(4)

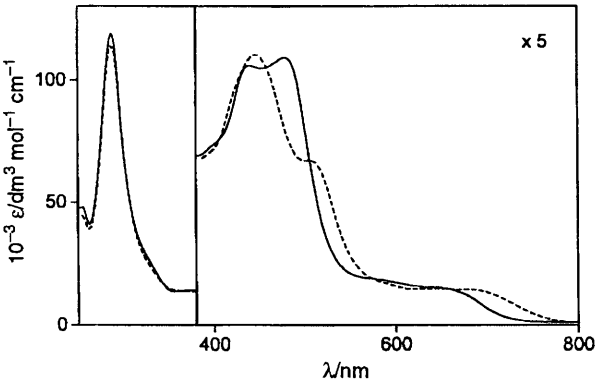

Fig. 3 Absorption spectra of Ru-LL'-Os (——) and Os-LL'-Ru (- - - -) in acetonitrile solution at room temperature

and homodinuclear M-LL'-M compounds (M = Ru or Os) are similar but not identical. In the mononuclear compounds the three ligands are almost equivalent {as shown by comparing the electrochemical behavior of the mononuclear compounds with that of $[Ru(bipy)_3]^{2+}$ and $[Os(bipy)_3]^{2+}$, Table 4}, so that the m.l.c.t. transitions involving the bipy and LL' ligands are very close in energy. This, however, is not the case for the dinuclear compounds where the electronic properties of the bridging ligand are different from those of the bipy ligands. More specifically, the electrochemical data show that in the dinuclear complexes the bridging ligand is much easier to reduce than bipy, and the metals are more difficult to oxidize than in the mononuclear compounds. Accordingly, the M ⟶ (LL') and M ⟶ (bipy) c.t. transitions, which are almost isoenergetic in the mononuclear compounds, are expected to move to the red and, respectively, to the blue in passing to the homodinuclear compounds.* Since the difference in energy is relatively small and most of the intensity is carried by the M ⟶ (bipy) c.t. transitions (around each metal there are two bipy ligands and only one bridging ligand moiety), the only change that is observed on passing from the mononuclear to the homodinuclear compounds is a small blue shift of the band maximum and the appearance of a shoulder on the low energy side of the absorption band. The spectra of the heterodinuclear Ru-LL'-Os and Os-LL'-Ru compounds (Fig. 3) exhibit several absorption features because of the simultaneous presence of Os- and Ru-based m.l.c.t. transitions (again involving the terminal bipy ligands and the bridging ligand).

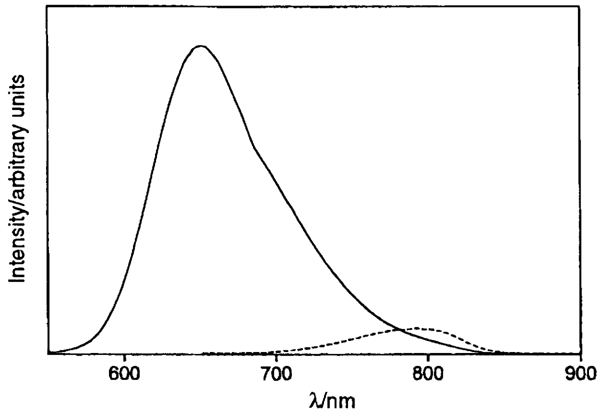

Fig. 4 Uncorrected luminescence spectra of isoabsorptive solutions (λ_{exc} = 469 nm) of Ru-LL'-Ru (——) and Os-LL'-Os (- - - -) in acetonitrile at room temperature

Luminescence Properties of the Mononuclear and Homodinuclear Complexes.—Most of the luminescence results are gathered in Table 6. The uncorrected luminescence spectra of Ru-LL'-Ru and Os-LL'-Os in acetonitrile solution at room temperature are shown in Fig. 4. Emission maxima, luminescence quantum yields, and excited-state lifetimes are in the expected range for triplet m.l.c.t. emission of Ru^{II} and Os^{II} bipy-type complexes.[2,3] Even in the heterodinuclear compounds, only one luminescence band and a single exponential decay are observed despite the electronic differences between the two metal fragments. The lowest excited states of the two co-ordination sites in the homodinuclear compounds Ru-LL'-Ru and Os-LL'-Os should have slightly different energies. The fact that only one band and a single exponential decay is observed in each case suggests either a fast equilibrium between these two states, or no communication but very similar properties of the two levels. In view of the sizeable metal-metal interaction shown by the electrochemical results and of the behaviour of the heterodinuclear compounds (see below), the first hypothesis is fully justified. According to the electrochemical data, the lowest (luminescent) excited state lies on the L co-ordination site.

The red shift of the emission maximum along the series $[Ru(bipy)_3]^{2+}$, Ru-LL' and Ru-LL'-Ru (Table 6) is in agreement with the electrochemical results. It is well known that the emission energy increases with increasing 'redox energy', ΔE_{redox}, obtained by subtracting the (first) ligand-centred reduction potential from the (first) metal-centred oxidation potential.[21] From the data shown in Table 4 one can see that the values of ΔE_{redox} are 2.61, 2.56 and 2.45 V, respectively, for the three compounds mentioned above; the corresponding emission maxima are at 16 300, 15 000 and 14 800 cm^{-1}. The relationship is not linear, the emission energy of Ru-LL' is much closer to that of Ru-LL'-Ru than it is to $[Ru(bipy)_3]^{2+}$, in contrast to the electrochemical data indicating perhaps that other subtle effects are at work here, but the general trend is as expected. The blue shift of the emission band in going from fluid solution at room temperature to rigid glasses at 77 K, related to the lack of solvent repolarization after the m.l.c.t. transition, is slightly smaller in the dinuclear than in the mononuclear compound, presumably because in the latter the reduced site (*i.e.*, the L moiety of the bridging ligand) is somewhat shielded towards solvent interaction. For the series $[Os(bipy)_3]^{2+}$, Os-LL' and Os-LL'-Os the relationship between ΔE_{redox} and emission energy is less well-defined, but it is well known that in the osmium compounds the degree of

---

* Even the two m.l.c.t. transitions involving the two different moieties of the bridging ligand have different energy, but the difference is too small to have appreciable consequences in the absorption spectra.

Table 4 Electrochemical data for the complexes[a]

Complex	M^{2+}–M^{3+} couples(s)	Ligand-based couples		
Ru–LL′	+0.90 (70)	−1.66 (60)	−1.89 (80)	−2.12 (70)
Ru–LL′–Ru[b]	+0.99, +1.06[c]	−1.46 (60)	−1.73 (60)	−1.86 (70)
Os–LL′	+0.47 (70)	−1.62 (60)	−1.85 (100)	−2.12 (100)
Os–LL′–Os	+0.56, +0.65[c]	−1.39 (60)	−1.63 (70)	−1.81 (60)
Ru–LL′–Os	+0.60 (60), +1.05 (70)	−1.43 (60)	−1.66 (60)	−1.85[d]
Os–LL′–Ru	+0.57 (70), +1.09 (80)	−1.42 (70)	−1.71[d]	−1.83[d]
[Ru(bipy)$_3$][PF$_6$]$_2$[e]	+0.89 (70)	−1.72 (60)	−1.92 (80)	−2.16 (80)
[Os(bipy)$_3$][PF$_6$]$_2$[e]	+0.46 (80)	−1.63 (80)	−1.81 (70)	−2.11 (70)

[a] Potentials are in V *vs.* ferrocene–ferrocenium couple; cyclic voltammetric peak–peak separations ΔE_p for chemically reversible processes are in parentheses where available. All measurements were made in distilled MeCN containing 0.1–0.2 mol dm^{-3} NBu$_4$PF$_6$, at a Pt-bead working electrode, with a scan rate of 0.2 V s^{-1}. [b] Taken from ref. 16. [c] Two (assumed reversible) metal-based oxidations not separable by cyclic voltammetry, so peak potentials taken from square-wave voltammogram. [d] Process not fully reversible or poorly resolved in cyclic voltammogram, so peak potentials taken from square-wave voltammogram. [e] Recorded under the same conditions for comparison.

Table 5 Electronic spectra of the complexes[a]

Complex	λ_{max}/nm (ε/dm^3 mol^{-1} cm^{-1})			
Ru–LL′	288 (74 000)	453 (13 300)		
Ru–LL′–Ru	286 (111 000)	448 (21 000)		
Os–LL′	290 (71 000)		480 (11 900)	650 (3 100)[b]
Os–LL′–Os	289 (118 000)		471 (21 000)	650 (5 700)[b]
Ru–LL′–Os	286 (118 000)	438 (21 000)	476 (22 000)	646 (2 700)[b]
Os–LL′–Ru	286 (114000)	446 (22 000)	509 (13 400)	690 (2 800)[b]
[Ru(bipy)$_3$]$^{2+}$[c]	288 (76 600)	452 (14 600)		
[Os(bipy)$_3$]$^{2+}$[c]	290 (78 000)	436 (10 700)	478 (11 100)	579 (3 300)

[a] In acetonitrile solution. [b] Broad absorption band. [c] From ref. 11.

Table 6 Luminescence properties of the complexes[a]

	298 K					77 K[b]			
	Ru		Os			Ru		Os	
Complex	λ/nm	τ/ns	λ/nm	τ/ns	Φ	λ/nm	τ/μs	λ/nm	τ/μs
Ru–LL′	666	191			1.5 × 10^{-2}	588	5.9		
Ru–LL′–Ru	674	232			1.9 × 10^{-2}	612	5.7		
Os–LL′			792	30	1.0 × 10^{-3}			722	1.3
Os–LL′–Os			814	21	8.8 × 10^{-4}			756	1.2
Ru–LL′–Os			756	41	3.2 × 10^{-3}			716	1.5
Os–LL′–Ru			808	26	1.3 × 10^{-3}			756	1.0
[Ru(bipy)$_3$]$^{2+}$[c]	615	170			1.5 × 10^{-2}	582	5.0		
[Os(bipy)$_3$]$^{2+}$[c]			743	49	3.2 × 10^{-3}			710	0.8

[a] In aerated acetonitrile solution at room temperature, unless otherwise noted. The emission maxima are taken from corrected spectra. [b] Butyronitrile solution. [c] From ref. 11, Φ from this work.

effective charge transfer is smaller than in the ruthenium compounds and the electrochemical–spectroscopic correlations are less clean.

Luminescence Properties of the Heterodinuclear Complexes.—In Ru–LL′–Os and Os–LL′–Ru the lowest excited-state level of the Ru-based moiety lies about 3000 cm^{-1} above the lowest excited-state level of the Os-based moiety (Table 5). In these complexes, only the Os-based luminescence can be observed, and the excitation spectrum (monitored at 750 nm) matches the absorption spectrum. Furthermore, no short-lived Ru-based luminescence can be observed, showing that the residual Ru-based emission (if any) has a too short lifetime and/or an intensity too weak to be revealed. In any case, these results show that energy transfer from the Ru- to the Os-based moiety has to be practically 100% efficient and fast compared to the limits of our apparatus, *i.e.* $k_{en} > 5 \times 10^8$ s^{-1}. By comparison with other systems, with a Ru ··· Os separation of 17 Å and a bicyclooctane unit included in the bridge to prevent direct conjugation between the metals, k_{en} values of *ca.* 5 × 10^7 s^{-1} were observed with energy-transfer efficiencies of *ca.* 90%.[11,12] Similarly a k_{en} value of 0.8 × 10^7 s^{-1} for Ru^{II} $\longrightarrow$ Os^{II} energy transfer across a cyclohexyl spacer has recently been reported.[22] Since the lack of a conjugated pathway is clearly no barrier to energy transfer, it is not surprising that energy transfer occurs with essentially 100% efficiency in Ru–LL′–Os and Os–LL′–Ru despite the near-orthogonality of the component parts, and the small metal–metal separation means that the real rate constant for the energy transfer may be very much higher than our lower limit.

The heterodinuclear compounds exhibit different Os-based emission properties, as expected because of the non-equivalence of the two co-ordination sites of the LL′ ligand. The Os-based emission from site L of Os–LL′–Ru is of lower energy than the Os-based emission from site L′ of Ru–LL′–Os. This is consistent with the electrochemical results which show that the Os^{II} centre is oxidised at a less positive potential when in site L. The elongation of one of the Os–N bonds at the more hindered site L′ with consequent decrease of the ligand field (l.f.) strength does not hamper emission from that site; in fact the Os-based luminescence quantum yield and emission lifetime at room temperature are both higher for site L′ than for site L. This behaviour is not surprising. In ruthenium(II)–polypyridine complexes the rate of the radiationless deactivation process (which competes with luminescence) increases on decreasing ligand-field strength because the most important deactivation path of the ^{3}m.l.c.t. level is *via* the upper lying ^{3}l.f. level.[2,3] In the osmium(II) complexes, however, the ligand-field strength is much higher than in ruthenium(II) complexes and the ^{3}m.l.c.t. level lies at lower energy. As a consequence, radiationless decay of the luminescent ^{3}m.l.c.t. level *via* the upper lying ^{3}l.f. level is prevented, and the luminescence properties are not so sensitive to distortions in the co-ordination sphere. The most important radiationless decay in osmium(II) complexes is that going directly to the ground state and is regulated by the energy gap between the ^{3}m.l.c.t. level and the ground state.[2,3,23] The luminescence lifetime and quantum yield decrease with decreasing energy of the ^{3}m.l.c.t. level in the series Ru–LL′–Os > Os–LL′–Ru > Os–LL′–Os (Table 6) according to the above expectation.

Conclusion

The results obtained from electrochemical experiments, absorption spectra, and luminescence investigations on the mononuclear and dinuclear compounds Ru–LL′, Os–LL′, Ru–LL′–Ru, Os–LL′–Os, Ru–LL′–Os and Os–LL′–Ru show that: (*i*) the two chelating sites of the 2,2′:3′,2″:6″,2‴-quaterpyridine bridging ligand LL′ are, as expected, non-equivalent; (*ii*) a metal ion is easier to oxidize when it occupies the L co-ordination site; (*iii*) in the dinuclear compounds the metal–metal interaction is not negligible; (*iv*) the lowest energy (luminescent) level in the dinuclear compounds is located on the L co-ordination site, consistent with the electrochemical data; (*v*) the difference in the properties of the two moieties of the LL′ bridging ligand is much smaller than the difference in the properties of Ru^{II} and Os^{II} metal ions, so that in the two mixed-metal complexes, Ru–LL′–Os and Os–LL′–Ru, the metal easier to oxidize is always Os and the luminescent moiety is always the Os-based one; (*vi*) in the two heterodinuclear compounds, electronic energy transfer from the higher energy to the lower energy moiety is very fast and 100% efficient.

Experimental

Proton NMR spectra were recorded on JEOL GX270 or GX400 spectrometers. Fast-atom bombardment (FAB) mass spectra were recorded on a VG-Autospec instrument with 3-nitrobenzyl alcohol as matrix. Electrochemical experiments were performed with an EG&G-PAR model 273A potentiostat. A standard three-electrode configuration was used with Pt-bead working and auxiliary electrodes and a saturated calomel electrode (SCE) reference; all potentials are quoted in V *vs.* the ferrocene–ferrocenium couple. The measurements were carried out on acetonitrile solutions of the complexes containing 0.1–0.2 mol dm^{-3} NBu_4PF_6 as supporting electrolyte.

Absorption spectra were recorded with a Perkin-Elmer Lambda 9 spectrophotometer in acetonitrile solution. Luminescence experiments were performed in acetonitrile solution at room temperature and in a butyronitrile rigid matrix at 77 K. Uncorrected luminescence spectra were obtained with a Spex Fluorolog II spectrofluorimeter. Correction of the luminescence intensity profile was performed either by using software provided by the firm or by employing a calibrated 45 W quartz-halogen tungsten filament lamp by Optronic Laboratories as a standard for the correction of the phototube response. Luminescence quantum yields were computed by comparing areas of corrected luminescence spectra on an energy scale, following the method described by Demas and Crosby[24] and using $[Ru(bipy)_3]^{2+}$ as a standard ($\Phi = 2.8 \times 10^{-2}$ in aerated water[25]). Luminescence lifetimes were obtained with an IBH single photon counting apparatus (N_2 lamp, 337 nm). The ligand LL′ and complexes Ru–LL′ and Ru–LL′–Ru were prepared as described earlier.[16,17] The compounds $[Ru(bipy)_2Cl_2]\cdot 2H_2O$ and $[Os(bipy)_2Cl_2]$ were prepared according to the standard literature methods.[26,27]

Syntheses.—$[Os(LL')(bipy)_2][PF_6]_2$ (Os–LL′). A mixture of $[Os(bipy)_2Cl_2]$ (0.24 g, 0.42 mmol) and LL′ (0.20 g, 0.64 mmol) was heated to reflux in ethylene glycol for 5.5 h to afford a dark green solution. After cooling and precipitation of the complex with aqueous KPF_6, the crude solid was filtered off, dried, and purified by column chromatography on alumina. Initial elution with acetonitrile–toluene (1:1) removed unreacted ligand; Os–LL′ was then eluted with neat acetonitrile (0.298 g, 64%).

$[(bipy)_2Os(LL')Os(bipy)_2][PF_6]_4$ (Os–LL′–Os). A mixture of $[Os(bipy)_2Cl_2]$ (0.554 g, 0.96 mmol) and LL′ (0.10 g, 0.32 mmol) was heated to reflux in ethylene glycol for 5.5 h to afford a dark green-brown solution. After precipitation and filtration as above, the crude product was purified by chromatography on alumina with acetonitrile–toluene (1:1). Traces of the mononuclear complex Os–LL′ eluted first; Os–LL′–Os was then eluted (0.346 g, 57%).

$[(bipy)_2M(LL')M'(bipy)_2][PF_6]_4$ (M = Ru, M′ = Os, Ru–LL′–Os; M = Os, M′ = Ru, Os–LL′–Ru). A mixture of M–LL′ (M = Ru or Os, 0.15 mmol) and $[M'(bipy)_2Cl_2]$ (M′ = Os or Ru, respectively, 0.15 mmol) was heated to reflux in ethlyene glycol for 3 h to give a dark solution. After precipitation with aqueous KPF_6 and filtration as above the crude material was purified by chromatography on alumina with MeCN–toluene (1:1), followed by recrystallisation from acetonitrile–diethyl ether (yields approx. 65% in both cases).

Analytical and mass spectroscopic data for the complexes are in Table 1.

Crystal Structure Determination of $[(bipy)_2Os(LL')Ru(bipy)_2][PF_6]_4\cdot 3MeCN$.—Dark green-brown crystals suitable for X-ray diffraction were grown from acetonitrile–diethyl ether by vapour diffusion. A suitable crystal (0.7 × 0.3 × 0.2 mm) was mounted in a capillary tube filled with mother-liquor to prevent loss of solvent of crystallisation. Crystal data: $C_{66}H_{55}F_{24}N_{15}OsP_4Ru$, $M = 1929.4$, monoclinic, space group $P2_1/n$, $a = 17.373(11)$, $b = 25.088(13)$, $c = 17.507(11)$ Å, $\beta = 106.15(5)°$, $U = 7329(8)$ Å^3, $Z = 4$, $D_c = 1.748$ Mg m^{-3}, $F(000) = 3808$. Intensity data were collected using a Siemens R3m/V diffractometer (293 K, Mo-Kα X-radiation, graphite monochromator, $\bar{\lambda} = 0.710\,73$ Å) in the range $4 < 2\theta < 45°$ by the Wyckoff ω-scan technique with index ranges $0 \leqslant h \leqslant 18$, $0 \leqslant k \leqslant 27$, $-18 \leqslant l \leqslant 18$. 9942 Reflections were collected of which 9573 were unique. The data were corrected for Lorentz, polarisation and X-ray absorption effects, the latter by an empirical method using azimuthal scan data ($\mu = 2.140$ mm^{-1}; min./max. transmission factors, 0.188, 0.255). Systematic monitoring of three check reflections at regular intervals showed no significant crystal decay. The structure was solved by conventional Patterson methods, and successive Fourier-difference syntheses were used to locate all non-hydrogen atoms. Hydrogen atoms were included in calculated positions (C–H = 0.96 Å) and refined isotropically as riding atoms; all other atoms were refined anisotropically. Initial calculations were performed on a DEC micro-Vax II computer with the SHELXTL PLUS system of programs.[28] The final least-squares refinements (on all F^2 data) were carried out on a Silicon Graphics Indigo R4000 computer using SHELXL-93.[29] Refinement converged at $wR_2 = 0.183$ (9573 data, 12 restraints, 1003 parameters). For comparison with more conventional refinements against F, $R_1 = 0.065$ using only data with $F > 4\sigma(F)$. The largest difference peak and hole in the residual electron density map were 1.293 and -1.282 e Å^{-3}, both in the vicinity of the Os atom. Atomic coordinates are in Table 2, and selected bond lengths and angles in Table 3.

Additional material available from the Cambridge Crystallographic Data Centre comprises H-atom coordinates, thermal parameters and remaining bond lengths and angles.

Acknowledgements

This work was supported by Ministero dell' Universitá e della Ricerca Scientifica e Tecnologica and Consiglio Nazionale della Ricerce (Progetto Strategico Tecnologie Chimiche Innovative), Italy, and by EPSRC. We thank Dr. K. MacNeil for recording the FAB mass spectra of the complexes, and Johnson Matthey for the loan of ruthenium and osmium metal salts.

References

1 V. Balzani and F. Scandola, *Supramolecular Photochemistry*, Ellis Horwood, Chichester, 1991.
2 A. Juris, V. Balzani, F. Barigelletti, S. Campagna, P. Belser and A. von Zelewsky, *Coord. Chem. Rev.*, 1988, **84**, 85; E. M. Kober, J. V. Caspar, B. P. Sullivan and T. J. Meyer, *Inorg. Chem.*, 1988, **27**, 4587, and references therein.
3 K. Kalyanasundaram, *Photochemistry of Polypyridine and Porphyrin Complexes*, Academic Press, London, 1992.
4 R. Grigg and W. D. J. A. Norbert, *J. Chem. Soc., Chem. Commun.*, 1992, 1300; R. Grigg, J. M. Holmes, S. K. Jones and W. D. J. A. Norbert, *J. Chem. Soc., Chem. Commun.*, 1994, 185; V. Goulle, A. Harriman and J.-M. Lehn, *J. Chem. Soc., Chem. Commun.*, 1993, 1034; P. D. Beer, O. Kocian, R. J. Mortimer and C. Ridgway, *J. Chem. Soc., Chem. Commun.*, 1991, 1460.
5 V. Balzani and F. Scandola, in *Comprehensive Supramolecular Chemistry*, ed. D. N. Reinhoudt, Pergamon, New York, vol. 10, in the press.
6 G. Denti, S. Campagna, S. Serroni, M. Ciano and V. Balzani, *J. Am. Chem. Soc.*, 1992, **114**, 2944; S. Serroni, G. Denti, S. Campagna, A. Juris, M. Ciano and V. Balzani, *Angew. Chem., Int. Ed. Engl.*, 1992, **31**, 1493.
7 For some recent papers, see: F. Scandola, M. T. Indelli, C. Chiorboli and C. A. Bignozzi, *Top. Curr. Chem.*, 1990, **158**, 73; J.-P. Collin, S. Guillerez, J.-P. Sauvage, F. Barigelletti, L. De Cola, L. Flamigni and V. Balzani, *Inorg. Chem.*, 1991, **30**, 4230; S. L. Mecklenburg, B. M. Peek, J. R. Schoonover, D. G. Mccafferty, C. G. Wall, B. W. Erikson and T. J. Meyer, *J. Am. Chem. Soc.*, 1993, **115**, 5479; W. E. Jones, jun., C. A. Bignozzi, P. Chen and T. J. Meyer, *Inorg. Chem.*, 1993, **32**, 1167; M. K. Nazeeruddin, A. Kay, I. Rodicio, R. Humphry-Baker, E. Müller, P. Liska, N. Vlachopoulos and M. Grätzel, *J. Am. Chem. Soc.*, 1993, **115**, 6382; E. H. Yonemoto, Y. I. Kim, R. H. Schmehl, J. O. Wallin, B. A. Shoulders, B. R. Richardson, J. F. Haw and T. E. Mallouk, *J. Am. Chem. Soc.*, 1994, **116**, 10 557.
8 For some recent papers, see: S. Van Wallendael and D. P. Rillema, *J. Chem. Soc., Chem. Commun.*, 1990, 1081; M. Furue, K. Maruyama, Y. Kanematsu, T. Kushida and M. Kamachi, *Coord. Chem. Rev.*, 1994, **132**, 201; K. Nokazaki and T. Ohno, *Coord. Chem. Rev.*, 1994, **132**, 215; S. Van Wallendael, M. W. Perkovic and D. P. Rillema, *Inorg. Chim. Acta*, 1993, **213**, 253.
9 J.-P. Gisselbrecht, M. Gross, J.-M. Lehn, J.-P. Sauvage, R. Ziessel, C. Piccinni-Leopardi, J. M. Arrieta, G. Germain and M. Van Meerssche, *Nouv. J. Chim.*, 1984, **8**, 661.
10 A. J. Downard, G. E. Honey, L. F. Phillips and P. J. Steel, *Inorg. Chem.*, 1991, **30**, 2259.
11 L. De Cola, V. Balzani, F. Barigelletti, L. Flamigni, P. Belser, A. von Zelewsky, M. Frank and F. Vögtle, *Inorg. Chem.*, 1993, **32**, 5228.
12 F. Vögtle, M. Frank, M. Nieger, P. Belser, A. von Zelewsky, V. Balzani, F. Barigelletti, L. De Cola and L. Flamigni, *Angew. Chem., Int. Ed. Engl.*, 1993, **32**, 1643.
13 A. C. Benniston, V. Grosshenny, A. Harriman and R. Ziessel, *Angew. Chem., Int. Ed. Engl.*, 1994, **33**, 1884.
14 F. Barigelletti, L. Flamigni, V. Balzani, J.-P. Collin, J.-P. Sauvage, A. Sour, E. C. Constable and A. M. W. Cargill Thompson, *Coord. Chem. Rev.*, 1994, **132**, 209; *J. Chem. Soc., Chem. Commun.*, 1993, 942.
15 L. De Cola, F. Barigelletti, V. Balzani, R. Hage, J. G. Haasnoot and J. Reedijk, *Chem. Phys. Lett.*, 1991, **178**, 491 and references therein.
16 M. D. Ward, *J. Chem. Soc., Dalton Trans.*, 1993, 1321.
17 D. A. Bardwell, F. Barigelletti, R. L. Cleary, L. Flamigni, M. Guardigli, J. C. Jeffery and M. D. Ward, *Inorg. Chem.*, 1995, **34**, 2438.
18 E. C. Constable, P. R. Raithby and D. N. Smit, *Polyhedron*, 1989, **8**, 367.
19 D. P. Rillema, D. S. Jones and H. A. Levy, *J. Chem. Soc., Chem. Commun.*, 1979, 849; J. M. Harrowfield and A. N. Sobolev, *Aust. J. Chem.*, 1994, **47**, 763.
20 CAChe work system, CAChe Scientific, Beaverton, OR, USA, 1994.
21 E. S. Dodsworth and A. B. P. Lever, *Chem. Phys. Lett.*, 1984, **112**, 567; A. A. Vlcek, E. S. Dodsworth, W. J. Pietro and A. B. P. Lever, *Inorg. Chem.*, 1995, **34**, 1906.
22 G. Giuffrida, G. Calogero, V. Ricevuto and S. Campagna, *Inorg. Chem.*, 1995, **34**, 1957.
23 J. M. Kelly, C. Long, C. M. O'Connell, J. G. Vos and A. H. A. Tinnemans, *Inorg. Chem.*, 1983, **22**, 2818; R. H. Fabian, D. M. Klassen and R. W. Sonntag, *Inorg. Chem.*, 1980, **19**, 1977.
24 J. N. Demas and G. A. Crosby, *J. Phys. Chem.*, 1971, **75**, 991.
25 K. Nakamura, *Bull. Chem. Soc. Jpn.*, 1982, **55**, 2697.
26 B. P. Sullivan, D. J. Salmon and T. J. Meyer, *Inorg. Chem.*, 1978, **17**, 3334.
27 M. J. Kendrick Geno and J. H. Dawson, *Inorg. Chim. Acta*, 1985, **97**, L41.
28 SHELXTL-PLUS: Software Package for the Determination of Crystal Structures, Siemens Analytical X-ray Instruments Inc., Madison, WI, 1990.
29 G. M. Sheldrick, SHELXL-93, Göttingen, 1993.

Received 10*th July* 1995; *Paper* 5/04476F